

MASTER

CONF-820828--8

NUCLEAR STRUCTURE IN PION SCATTERING AND CHARGE EXCHANGE

DE83 007945

Benjamin ZEIDMAN and Donald F. GEESAMAN

Argonne National Laboratory, Argonne, IL 60439, USA

Abstract: Data from pion inelastic scattering and charge-exchange experiments are discussed within the framework of a DWIA analysis. The properties of the pion-nucleon interaction transformed to the pion-nuclear system are used to infer new nuclear-structure information for both discrete states and giant resonances.

1. Introduction

In recent years considerable data resulting from studies of the interactions of pions with nuclei have been generated at LAMPF, SIN, and TRIUMF. While much of this information involves the propagation of pions through the nuclear medium and the study of reaction mechanisms, a substantial fraction of the effort is related to investigation of nuclear structure. Comprehensive reviews¹⁾ of results from pion scattering and charge exchange have been presented at various conferences. Rather than being a comprehensive review or a summary of recent results, the present contribution focusses upon several new studies exhibiting particular aspects of nuclear structure that are well suited to investigation by pion scattering and charge exchange reactions.

At incident energies of approximately 180 MeV, pion induced reactions are dominated by the $T = 3/2, J = 3/2$ resonance in the π -nucleon system. The π -N amplitude then can be written in the form

$$f(k, k') = a(k) \left[\frac{2 - \vec{t} \cdot \vec{t}'}{3} \right] [2 \cos \theta + i \vec{\sigma} \cdot \vec{n} \sin \theta] \quad (1)$$

where $a(k)$ contains the energy dependence of the interaction, \vec{t} and \vec{t}' are the isospins of the pion and nucleon, respectively, θ is the scattering angle, and \vec{n} is normal to the scattering plane. It has been shown that the π -nucleus interaction has a similar form²⁾ except that $a(k)$ exhibits a weaker energy dependence and τ refers to the nuclear state. We see that isoscalar amplitudes are favored over isovector amplitudes because of the isospin term and that natural parity transitions are favored over spin-dependent transitions at small scattering angles.

Since the interaction near resonance is quite strong, the nucleus is highly absorptive and only the surface region is particularly amenable to study by pion scattering and charge exchange. As is generally found in strong absorption regimes, this leads to simplifications in the treatment of reaction mechanisms and reduces the dependence upon the details of pion interactions in the nuclear medium. In this contribution we consider pion scattering and charge exchange only in the resonance region so that nuclear structure dependent features may be emphasized.

2. Theoretical Considerations

The extraction of nuclear structure information from pion scattering and charge exchange requires a theoretical framework for analysis of the data. A particularly useful approach is that

NOTICE

PORTIONS OF THIS REPORT ARE ILLEGIBLE. It has been reproduced from the best available copy to permit the broadest possible availability.

EAC

DISCLAIMER

This report was prepared as an account of work sponsored by an agency of the United States Government. Neither the United States Government nor any agency thereof, nor any of their employees, makes any warranty, express or implied, or assumes any legal liability or responsibility for the accuracy, completeness, or usefulness of any information, apparatus, product, or process disclosed, or represents that its use would not infringe privately owned rights. Reference herein to any specific commercial product, process, or service by trade name, trademark, manufacturer, or otherwise does not necessarily constitute or imply its endorsement, recommendation, or favoring by the United States Government or any agency thereof. The views and opinions of authors expressed herein do not necessarily state or reflect those of the United States Government or any agency thereof.

COMMENCEMENT
OF TEXT

developed by Lee and Kurath³⁾ to treat pion inelastic scattering at energies near the (3,3) resonance. They incorporate shell-model wavefunctions into a framework of a first-order distorted-wave impulse approximation (DWIA) formulated in momentum space. The particle-hole excitations involved in inelastic scattering are described in the LS representation where the p-h orbital angular momenta are coupled to L, the spins to S, and total angular momentum J. They obtain transition amplitudes of the form

$$T_{fi} = \int t_{\pi N}(k', k, J, L, S, \omega) F_{fi}^N(J, L, S). \quad (2)$$

In this factorized form, $t_{\pi N}$ is the pion-nucleon collision matrix and F_{fi}^N is the nucleon transition density for inelastic excitation from state i to final state f. The collision matrix contains all of the dynamics of the pion-nucleus interaction including the dependence upon angular momentum coupling, energy dependence of the π -nucleon interaction, and angular dependence. The transition density describes the specifically nuclear properties of the transition, independent of probe.

In principle, many terms contribute to the sum in eq. (2), but calculations have shown that, for strong transitions, only one term usually dominates for a given J. In addition, near resonance, except for the isospin dependence of the interaction, the single particle-hole cross sections for π^+ and π^- scattering on light nuclei are nearly equal. It is therefore valid to approximate the differential cross sections for inelastic scattering by

$$\frac{d\sigma}{d\Omega}(\pi^+, \theta) \approx C_{JLS}(\theta) \left(\frac{2I_f + 1}{2I_i + 1} \right) (3F_{fi}^p(J) + F_{fi}^n(J))^2 \quad (3)$$

and

$$\frac{d\sigma}{d\Omega}(\pi^-, \theta) \approx C_{JLS}(\theta) \left(\frac{2I_f + 1}{2I_i + 1} \right) (F_{fi}^p(J) + 3F_{fi}^n(J))^2, \quad (4)$$

where $C_{JLS}(\theta)$ is the intrinsic "single particle" differential cross section, $I_{f(i)}$ are the final (initial) nuclear spins and $F_{fi}^{p(n)}$ are the proton (neutron) transition densities. Contributions from different values of J are summed incoherently. The explicit isospin dependence of the (3,3) resonance appears as the factors of 3 in eqs. (3) and (4). The complete DWIA calculations take absorption, distortion, spin and isospin dependence into account. The partial wave amplitudes for these calculations are obtained from analysis of pion elastic scattering.

As a consequence of the strong absorption, each $C_{JLS}(\theta)$ has a distinctive angular distribution that is typical of diffraction. In fig. 1 the most important angular distributions are shown. Indeed, many of the qualitative features seen in fig. 1 are similar to those of angular distributions obtained in alpha particle scattering and in heavy-ion reactions. With increasing multipolarity, the maxima of the angular distributions appear at larger scattering angles corresponding to larger momentum transfer, q. The exception is the 1(1,1) transition, spin-flip electric dipole, which, in contrast to all other spin-flip transitions, exhibits a peak at zero degrees. This phenomenon has recently been shown to be a theoretical consequence of strong absorption⁴⁾ and, as seen in fig. 2, has also been observed experimentally.⁵⁾

The relative importance of spin-flip amplitudes is also observed in fig. 1 where it is seen that the magnitudes of the magnetic multipoles not only are comparable to the natural parity, i.e.

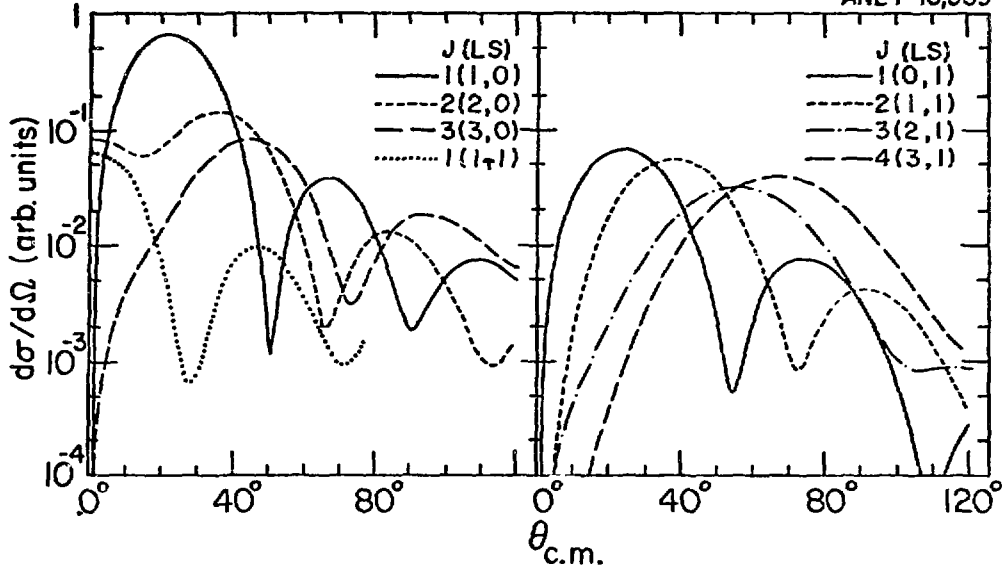


Fig. 1. Theoretical angular distributions, $C_{J,L,S}(\theta)$ for various values of J , L and S . The strong transitions are shown. On the left side, the angular distributions correspond to the electric transitions, $E1$, $E2$, $E3$ and $E1$ with spin-flip, while on the right side the magnetic transitions, $M1$, $M2$, $M3$ and $M4$ are shown. The calculations are appropriate for pion scattering by ^{11}B at $T_\pi = 162$ MeV.

electric, multipoles but that the intrinsic cross sections do not decrease rapidly with increasing multipolarity. An explanation of this effect in terms of the q -dependence of the π -nucleon interaction near resonance has been provided by Petrovich and Love.⁶⁾

Implicit in the DWIA formalism is a method for distinguishing spin-flip from non-spin-flip transitions. Siciliano and Walker²⁾ have expressed the DWIA cross section in a form similar to eq. (1), in which these two amplitudes are explicitly separated. For fixed momentum transfer, q_0 , near the primary maximum of the angular distribution their expression is

$$\frac{d\sigma}{d\Omega}(q_0, E, \theta) = \Gamma(E) [4M^2(q_0) \cos^2\theta + S^2(q_0) \sin^2\theta] \quad (5)$$

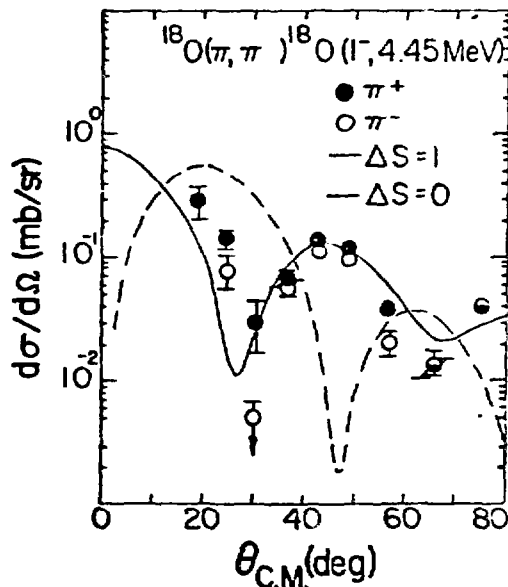


Fig. 2. Angular distributions for π^+ and π^- scattering to the 4.45-MeV 1^- state in ^{18}O .

COMMENCEMENT
OF TEXT

where $\Gamma(E)$ is an energy-dependent factor that is roughly constant in the vicinity of the resonance and θ is the scattering angle at energy E . M and S are spin-independent and spin-dependent form factors, respectively, that vary slowly with energy for momentum transfers near q_0 . For fixed q_0 , the energy dependence of the cross section will be governed by the dominance of either M^2 or S^2 thereby leading to a $\cos^2\theta$ dependence for non-spin-flip transitions or a $\sin^2\theta$ dependence for spin-flip transitions. Examples of the energy dependence of both types of transitions are shown in fig. 3 together with results of a DWIA calculation. The excitation functions are seen to verify the qualitative energy dependences predicted.

We therefore see that at pion kinetic energies near the (3,3) resonance the DWIA framework provides several tools for the extraction of nuclear structure information from pion scattering and charge exchange:

1. The isospin dependence of the pion-nucleon interaction is reflected in the pion-nucleus interaction to provide enhanced sensitivity for proton (neutron) transition densities in $\pi^+(\pi^-)$ scattering. In addition, the isospin dependence of the pion-nucleus interaction results in a factor of 2 enhancement of isoscalar transition amplitudes relative to isovector transition amplitudes.
2. Angular distributions of scattered pions have distinctive shapes that are determined by total angular momentum J , orbital angular momentum L , and spin dependence S .
3. Excitation functions taken at fixed momentum transfers corresponding to the maxima of angular distributions vary as $\cos^2\theta$ for natural-parity transitions and as $\sin^2\theta$ for spin-flip transitions, in analogy to the Rosenbluth formulae used in analysis of electron scattering.

In the following sections, these tools will be utilized in the analysis of several recent studies of pion scattering and charge exchange in which new nuclear structure information is obtained.

3. Inelastic Scattering by ^{11}B

An example is the analysis of the inelastic scattering of 162-MeV pions by ^{11}B which has been studied at EPICS by a collaboration from several institutions.⁸⁾ Spectra for π^+ and π^- scattering at 70° are shown in fig. 4. As is expected for a $T = 1/2$ nucleus, cross

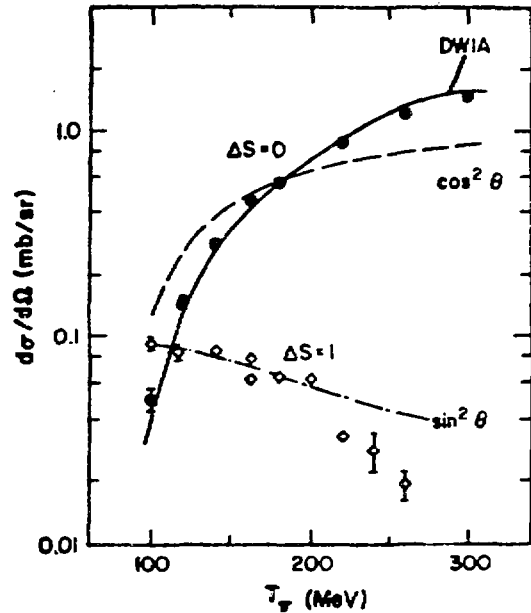


Fig. 3. Excitation function at constant q for the $3/2^-$ (solid points) and $9/2^-$ (open points) states in ^{13}C . The data⁷⁾ obtained at LAMPF with the use of the EPICS system.

COMMENCEMENT
OF TEXT

sections for inelastic pion scattering are different for π^+ and π^- , reflecting the variations in proton and neutron contributions to the transition densities. In contrast, the cross sections for elastic scattering of π^+ and π^- , shown in fig. 5, are equal and in reasonable agreement with momentum space optical model calculations.

The data for the inelastic scattering are analyzed using the approach of Lee and Kurath³⁾. For the low-lying negative parity states in ^{11}B , the Cohen-Kurath wavefunctions¹⁰⁾ are used to calculate transition densities. Angular distributions for several low-lying transitions are shown in fig. 6 together with the results of DWIA calculations for $2(2,0)$, i.e. E2, transitions. It is seen that the calculated shapes of the angular distributions are in good agreement with the data. The absolute magnitudes of the calculations, however, have to be increased to fit the data, i.e. the data indicate that the transitions are enhanced relative to calculations performed with a 1p-shell basis. This need for enhancement has long been known to exist in calculations of electromagnetic transition rates, and the enhancement factors required here are similar. Although the electromagnetic transitions are known to involve predominantly M1 amplitudes, the DWIA calculations indicate that even with no E2 enhancement the M1 terms contribute less than 10% of the cross section at the peak. This illustrates the effect of the π -nucleon interaction which favors natural parity transitions at relatively small scattering angles.

Quite prominent in the spectra shown in fig. 4 are a series of positive-parity states whose spins are indicated. Angular distributions for these states are displayed in fig. 7 together with excitation functions at two fixed momentum transfers. It is quite apparent from the data that the cross section for π^- scattering is larger than the π^+ cross section for each state and that the π^- to π^+ cross section ratio increases with increasing spin. Indeed, there is no evidence for the $11/2^+$ state in π^+ scattering. From the isospin dependence of π -nucleus interaction, the larger π^- cross sections are clear evidence that the transitions to these states involve mainly neutron excitations.

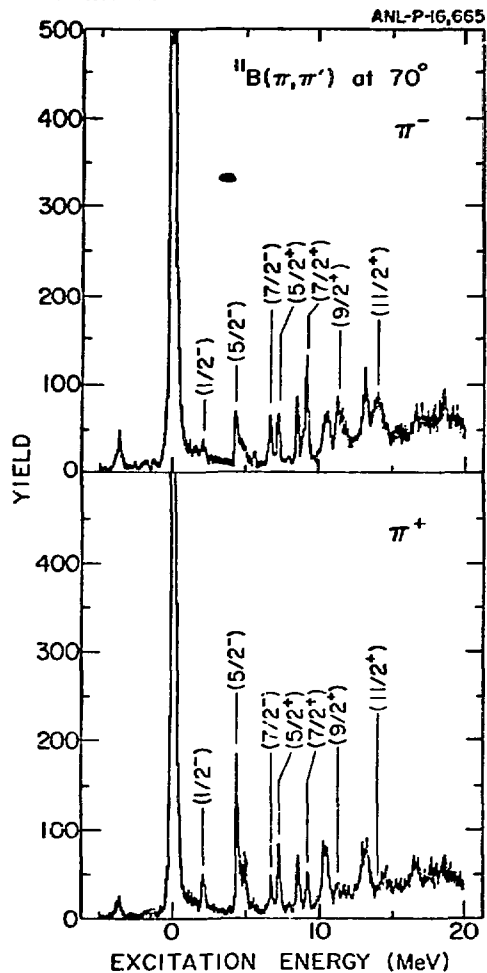


Fig. 4. Spectra for π^+ and π^- scattering for $T_\pi = 162$ MeV. Only levels discussed in the text are indicated. The yields indicate relative cross sections with the same normalization in both parts of the figure.

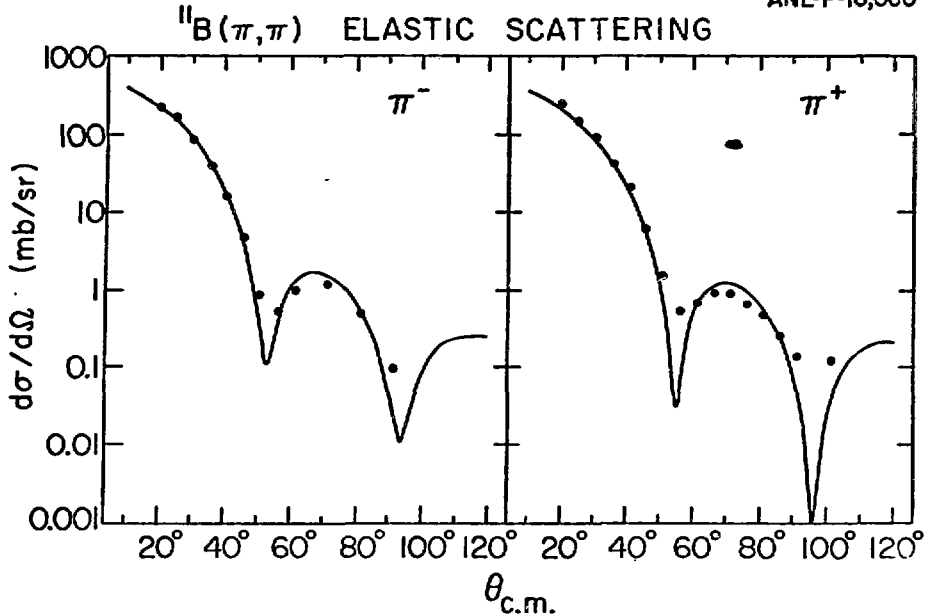


Fig. 5. Elastic scattering of pions at $T_{\pi} = 162$ MeV. The curves are the results of optical-model calculations using the code PIPIT.⁹⁾ Quadrupole contributions, not included in the calculations, are responsible for filling in the minima in the data.

The transition to the $11/2^+$ state at 14.04-MeV excitation must involve purely neutron excitation in order to conserve angular momentum i.e., a $d_{5/2}$ neutron coupled to the 3^+ ground state of ^{10}B . The particle-hole coupling therefore must be $4(31)$, in the notation of Section 2, and be the $(1p_{3/2}^{-1}, 1d_{5/2}^1)_4^-$ stretched configuration with multipolarity M4. Although the $11/2^+$ state is not seen in the π^+ scattering, the background is sufficient to permit a 9:1, π^-/π^+ ratio, consistent with a pure neutron excitation.

The positive parity states in ^{11}B result primarily from excitations of $1p$ -shell particles into the $1d_{2s}$ shell. Modified Millener-Kurath wavefunctions¹¹⁾ were used in the DWIA calculations shown in fig. 7 as solid lines. The dotted lines shown for the 9.2-MeV doublet are the calculated cross sections for the $5/2^+$ state at 9.27-MeV excitation while the light dashed lines are those for the $7/2^+$ state at 9.19-MeV excitation. With the exception of the curve for the $11/2^+$ state, the magnitudes of the calculated angular distributions have not been adjusted to fit the data; also shown is a 30% reduction in the calculation for π^- scattering to the 11.29-MeV state. In contrast to the agreement in magnitude found for the lower spin states, a normalization of 0.2 is required for the M4 calculation for the $11/2^+$ state. The transitions to the other positive parity states shown in fig. 7 are dominated by $3(30)$, E3, amplitudes.

Excitation functions were obtained at two fixed momentum transfers, $q = 1.1 \text{ fm}^{-1}$, the maximum of the E3 transition and $q = 1.5 \text{ fm}^{-1}$, the maximum of the M4 transition. For π^- , the qualitative behaviors shown in fig. 7 are consistent with the $\sin^2\theta(\text{E3})$ and $\cos^2\theta(\text{M4})$ energy dependences for non-spin-flip and spin-flip

COMMENCEMENT
OF TEXT

transitions, respectively. For π^+ at $q = 1.5 \text{ fm}^{-1}$, however, this is not the case and the excitation functions are similar to those observed in the minima of natural parity transitions. From these excitation function data at $q = 1.5 \text{ fm}^{-1}$, values may be obtained for the M4 contributions to π^- scattering to the $5/2^+$, $7/2^+$ and $9/2^+$ states. These have been added to the predicted angular distributions with the results being displayed as the heavy dashed lines in fig. 7. Substantially improved agreement with the data is observed. The M4 cross sections for the $5/2$, $7/2$ and $9/2$ states are approximately equal, with each being nearly equal to the cross section for the M4 transition to the $11/2^+$ state.

The extraction of M4 contributions to predominantly E3 transitions observed in π^- scattering together with the absence of such contributions in π^+ scattering indicates that neutrons are primarily involved. This result illustrates the utilization of the spin and isospin structure of the pion-nucleus interaction to infer different multipole admixtures in proton and neutron transition densities.

In view of the good agreement between the data and the theoretical predictions for the E3 transitions, the weakness of the M4 transition to the 14.04-MeV state is puzzling. While fragmentation of the strength into other $11/2^+$ states is possible through residual interactions, no other $11/2^+$ states have as yet been identified. Moreover, the presence of substantial M4 strength to the lower spin states is not easily understood.

In a recent publication¹²⁾, the $5/2^+$, $7/2^+$, $9/2^+$, $11/2^+$ sequence is considered as a rotational band and found to behave rather peculiarly. One description, contrary to the present data, involves 3 particle-3 hole excitations. An alternative description using one particle-hole excitations requires large oblate or triaxial deformations. In this latter picture, the band terminates at $11/2^+$ and the one particle in the 2s1d shell must be a neutron. The larger cross sections for π^- scattering to the band suggest further theoretical and experimental study.

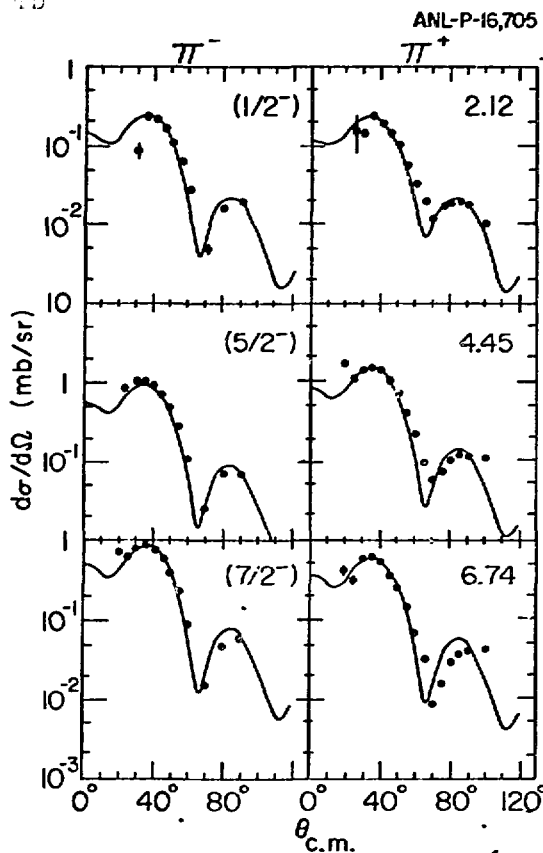


Fig. 6. Angular distributions for inelastic pion scattering to negative parity states in ^{11}B . The spins are indicated in the left panel while the excitation energies, in MeV, are indicated on the right. The curves are discussed in the text.

COMMENCEMENT
OF TEXT

TYPE IN SINGLE LINE SPACING WITHIN
THE FRAME PROVIDED

ANL-P-16,709

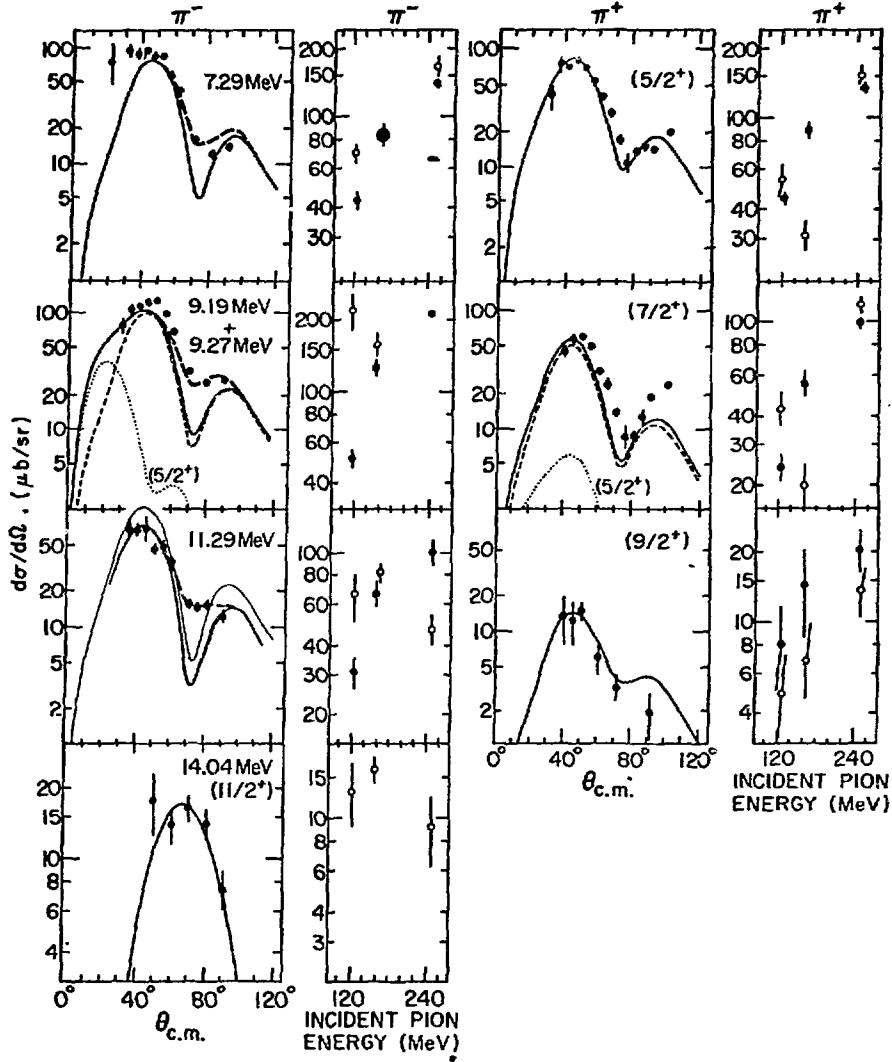


Fig. 7. Angular distributions for elastic pion scattering to positive-parity states in ^{11}B and excitation functions at constant momentum transfer, q . The excitation energies of the states are shown in the left-hand panel with corresponding spins toward the right. The curves are discussed in the text. The excitation functions shown correspond to $q = 1.1 \text{ fm}^{-1}$ (solid points) and $q = 1.5 \text{ fm}^{-1}$, (open points). For π^- , the open points are plotted at $5\times$ their true value, except for the $11/2^+$. For π^+ , the open points are plotted at $2\times$ the correct value.

4. 8^- States in ^{54}Fe

In the previous section, an anomalously low cross section for an M4, stretched transition was discussed. This is an example of an

COMMENCEMENT
OF TEXT

important problem involving excitation of the spin degrees of freedom in nuclei. There is now considerable evidence from (e,e'), (p,p') and (p,n) reactions^{13,14} indicating isovector spin excitations of nuclei are quenched, i.e. weaker than predicted. Several explanations, including the possible importance of Δ -hole states in spin-flip reactions, have been proposed^{13,15}. Significant tests of these mechanisms involve both the angular momentum dependence and the q dependence of the quenching. Stretched transitions consist of $1h\omega$ particle-hole excitations where both the particle and hole have $j = l+1/2$ coupled to the maximum angular momentum. Such states have been seen near closed shells where the degrees of freedom are limited and the level density for high spin states with unnatural parity is low. The particular interest in stretched states arises from their high spin, simple nuclear structure, and low probability for excitation through multi-step processes. Despite this apparent simplicity, in studies utilizing various probes, electrons and hadrons, only about 50% of the one particle-one hole strength is observed¹⁶ in isovector stretched transitions.

In contrast to electrons, which excite isovector transitions, and protons, for which isovector and isoscalar transition strengths are about equal, pions preferentially excite isoscalar transitions. There is, however, no systematic structure information concerning isoscalar spin-flip excitations. In the few cases studied, namely 6^- states observed in proton scattering¹⁷⁾ by ^{24}Mg and ^{28}Si and pion scattering¹⁸⁾ by ^{28}Si , the isoscalar strength is quenched even more than the isovector strength, being reduced by an additional factor of approximately two. Quenching mechanisms such as Δ -hole states are predicted to be weak for high-spin states and cannot cause isoscalar quenching.

It is more difficult to study isoscalar amplitudes in heavier nuclei since the neutron excess generally permits more than one isospin amplitude to contribute to inelastic scattering. Both isoscalar and isovector amplitudes contribute to the excitation of the 8^- , stretched states in ^{54}Fe that result from $(g_{9/2}, f_{7/2}^{-1})_8^-$ particle-hole excitations. These states have been studied¹⁹⁾ by scattering 162-MeV pions at EPICS and spectra for both π^+ and π^- scattering are shown in fig. 8.

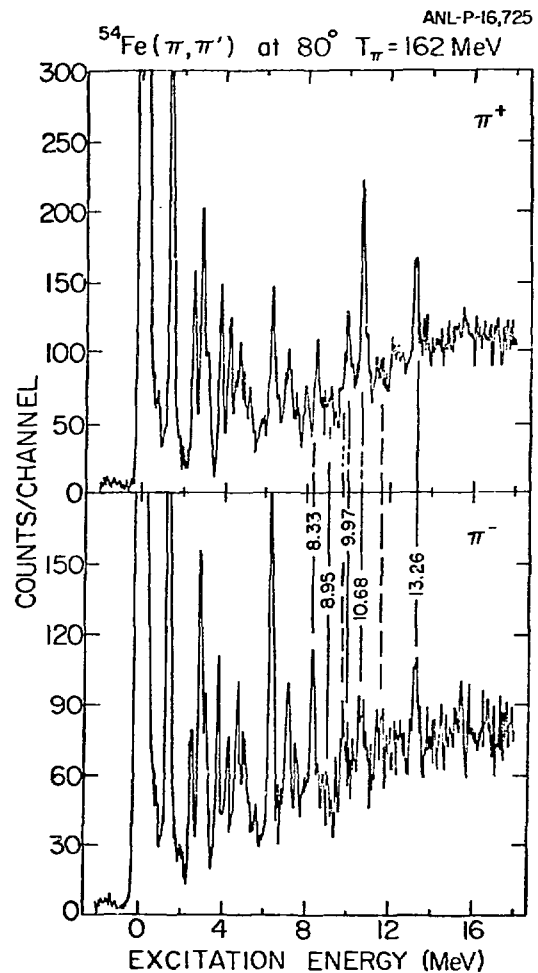


Fig. 8. Spectra for pion inelastic scattering by ^{54}Fe . The solid lines indicate M8 transitions observed in electron scattering. The vertical scales are normalized to the relative cross sections.

COMMENCEMENT
OF TEXT

In both spectra, there are a SINGLE LINE SPACING WITHIN

number of states that project above background at excitation energies greater than 8 MeV. M8 transitions have been observed in ^{54}Fe in electron scattering²⁰⁾ at the excitation energies indicated in the figure. Additional 8^- states are seen at the locations of the dashed lines. Because of the high background and limited counting statistics, weak peaks could not be identified as 8^- states; the background causes a minimum error of $2 \mu\text{b/sr}$ for π^+ and $3 \mu\text{b/sr}$ for π^- . Angular distributions for several 8^- states are shown in fig. 9 together with DWIA calculations for 8^- states. The wavefunctions used are obtained from shell-model calculations²¹⁾ constructed in the model space $(f_{7/2}^{-3}g_{9/2})$. The magnitudes of the cross sections are adjusted to fit the data.

The residual interactions cause fragmentation of the strength among the various 8^- states that can be constructed from configurations of the form $(f_{7/2}^{-3}g_{9/2})$. Shell-model calculations using this form have been reported²⁰⁾ and applied to electron scattering data. For electrons, only the isovector amplitude is important, while both isoscalar and isovector amplitudes are significant in pion scattering. In transitions to $T = 2$ states only the isovector amplitude contributes, so that π^+ and π^- cross sections should be equal except for minor Coulomb corrections. In fig. 9, it is seen that the π^+ and π^- cross sections for the 13.26-MeV state are equal, thereby confirming a $T = 2$ assignment for this state. For $T = 1$ states, however, the presence of both isoscalar and isovector amplitudes together with the isospin structure of the pion-nucleus interaction results in different π^+ and π^- cross sections. Indeed, in fig. 8 no trace of the 8.33-MeV state is seen in π^+ scattering while the peak is prominent in π^- scattering. On energetic grounds, a primarily neutron particle-hole excitation is expected since a neutron hole in ^{54}Fe forms a $T = 1/2$ state in the $(f_{7/2}^{-3})$ configuration while a proton hole makes only $T = 3/2$ states. In addition to the states previously observed, 8^- transitions are seen at excitation energies of 9.7 MeV and 11.7 MeV in π^- scattering and possibly at 11.7 MeV in π^+ scattering. No peak is seen at an excitation energy of 8.95 MeV where an 8^- state is reported in

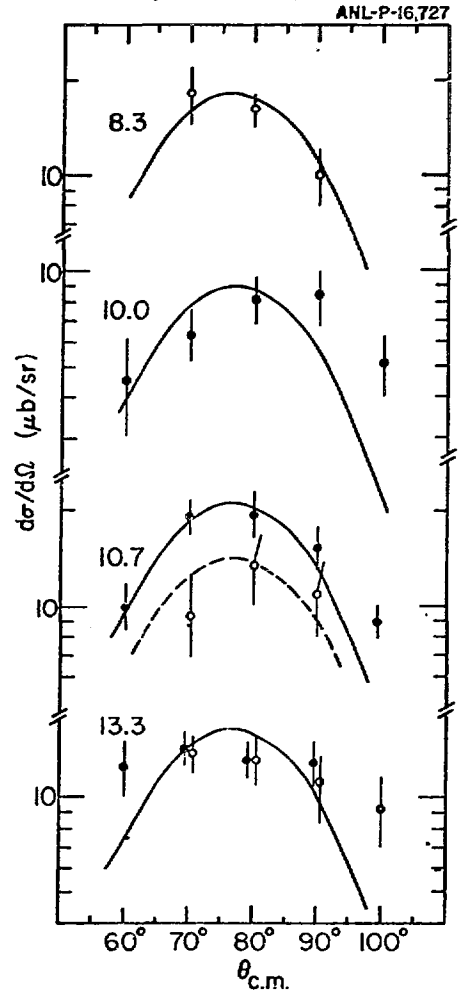


Fig. 9. Angular distributions for 8^- states from pion inelastic scattering by ^{54}Fe . The open points indicate π^- data while the solid points signify π^+ data. The curves are DWIA calculations discussed in the text.

COMMENCEMENT
OF TEXT

electron scattering.

The theoretical predictions for relative cross sections are compared to the data in fig. 10, together with electron scattering results. In fig. 10 the theoretical M8 strengths are plotted at the calculated excitation energies. The theoretical M8 electron transition strengths presented here²¹⁾ differ from those reported previously²⁰⁾ as a result of an adjustment to the strength of the isospin splitting designed to place the T = 2 state at the correct excitation energy. This adjustment results in improved agreement with the data for transition strengths, but causes shifts in the calculated excitation energies that make the establishment of correspondence to the data less direct.

The comparison of the model with the pion data shown in fig. 10 exhibits a consistent trend - all cross sections to the T = 1 states are overpredicted. It has already been noted, however, that isoscalar transitions in lighter, T = 0 nuclei are quenched relative to isovector transitions. Accordingly, the isoscalar amplitudes in the theoretical calculation for the 8⁻ transitions were reduced by a factor of 1/2 relative to the isovector amplitudes. The results of the calculation are shown as the heavy bars in fig. 10. It is seen that substantially better agreement with the experimental cross sections is obtained. Quite significantly, the states predicted to be quite strong at excitation energies between 11.5 and 12.0 MeV are reduced more than the other states in accord with the observed spectra.

It therefore seems probable, albeit indirectly, that the isoscalar transition amplitude is quenched relative to the isovector amplitude in ⁵⁴Fe. Whether this is generally true for heavier nuclei is an important issue, worthy of additional study both theoretically and experimentally. As the various questions concerning isovector excitation of spin degrees of freedom are clarified, the subject of quenching in isoscalar amplitudes will continue to be an area eminently suited to study by pion scattering.

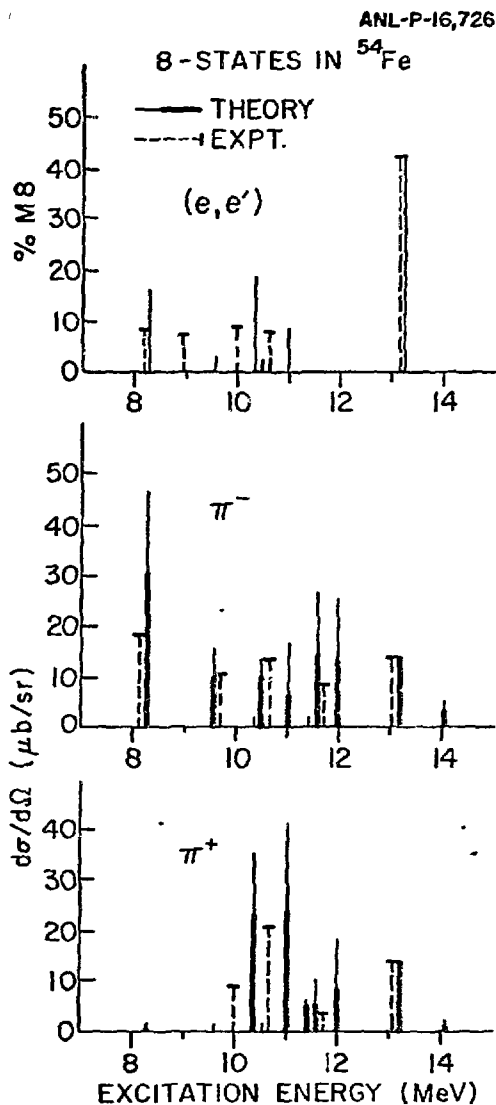


Fig. 10. Peak cross sections for 8⁻ states in π⁺ and π⁻ scattering. Also shown are data from electron scattering. The theoretical values discussed in the text are normalized to the data for the T = 2 state at 13.26 MeV excitation.

COMMENCEMENT
OF TEXT5. Giant Resonances
THE FRAME PROVIDED

In the previous sections, nuclear excitations leading to discrete final states were described in terms of single nucleon particle-hole configurations. Most of the nuclear response, however, is governed by collective excitations that involve many nucleons. These giant resonances are the normal modes of the nuclear medium and have been studied extensively; a session of this conference is devoted to this subject. Despite the more complicated radial dependences, the features of the pion-nucleon interaction still provide a selective means for the study of giant resonance phenomena and elucidation of nuclear structure information. Because of the multiparticle aspects, excitation of giant resonances in pion reactions may not be localized in the nuclear surface and medium corrections²²⁾ to the π -nucleon interaction may be important. These questions may be resolved in studies of the E1 and E2 resonances. The present discussion, however, will concentrate upon degrees of freedom whose identification results from the selectivity of pion interactions with nuclei. Inasmuch as pion charge exchange results²³⁾ are being presented at this conference, the discussion of this subject is somewhat abbreviated.

5.1 SPIN-FLIP EXCITATIONS IN ^{12}C

In a recent study of forward angle pion inelastic scattering²⁴⁾ by ^{12}C , prominent peaks were observed at excitation energies of 20-28 MeV. This structure is seen in the spectra of Fig. 11 together with a decomposition into several peaks. Angular distributions for the

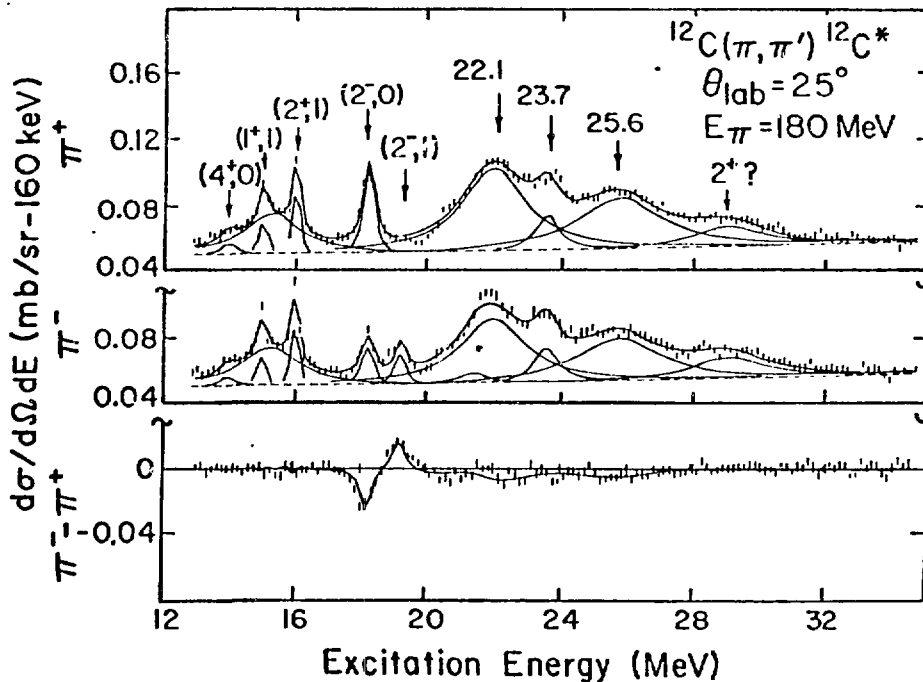


Fig. 11. Spectra for inelastic pion scattering by ^{12}C . Evidence for isospin mixing between the 2^- states near 19-MeV is seen in the lower part of the figure.

COMMENCEMENT
OF TEXT

TYPE IN SINGLE LINE SPACING WITHIN
OVERLAP

ANL-P-16,706

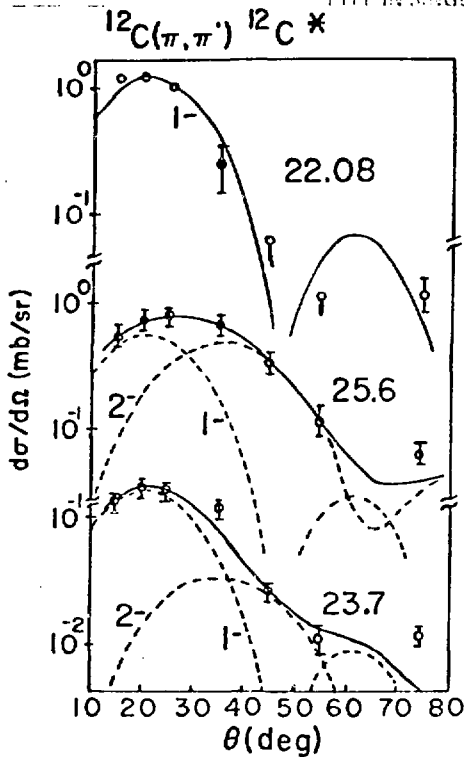


Fig. 12. Averaged π^+ and π^- angular distributions for the gross structure peaks at the indicated excitation energy. The curves are the results of DWIA calculation discussed in the text.

components of the decomposition are shown in Fig. 12 together with the results of DWIA calculations. For the 22.1-MeV peak, DWIA calculations with a $1(10)$, i.e. $E1$, shape are consistent with the data. Indeed, the isovector giant dipole resonance is known to peak at this energy. More interesting, however, are the shapes of the angular distributions for the other two peaks. In order to achieve agreement with the data, contributions with $2(1,1)$, i.e. $M2$, shapes have to be added to the $E1$ shape. While some $E2$ strength has been observed in this excitation energy region, the authors claim this is insufficient to provide much of the strength required. In addition, excitation functions rise too slowly with energy when compared to the rapid increase expected for natural parity excitations. This supports the suggestion that 2^- excitations provide the additional strength. From the DWIA analysis, it appears that a major fraction of the $E1$ strength is observed, but only a fraction of the total spin-flip 2^- strength is seen.

Quite recently, scattering of pions by ^{12}C has been studied at far forward angles²⁵⁾. Preliminary results are the spectra shown in

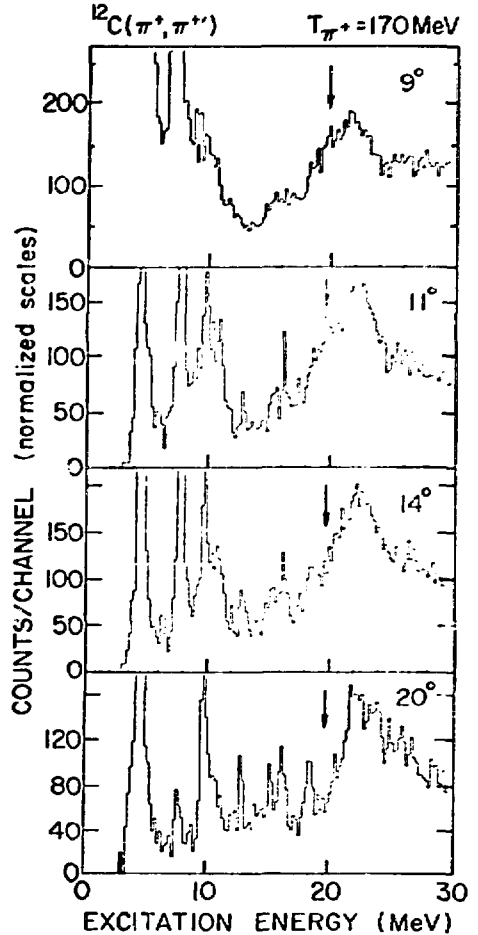


Fig. 13. Spectra for π^+ scattering at far forward angles. The vertical axes have been normalized to correspond to the relative yields. The arrow indicates the location of a 1 -excitation discussed in the text.

COMMENCEMENT
OF TEXT

Fig. 13. Since the scales are normalized, the heights of the peaks indicate relative cross section. The arrow indicates the location, approximately 19.6 MeV excitation, of a peak that is quite strong at 9° and decreases in intensity until it disappears into the background at 20° where the spectrum is quite similar to those in Fig. 11. This forward peaking behavior is characteristic of the 1(11), i.e. spin-flip E1, excitation mentioned in section 2. No other transition can exhibit such an angular distribution in inelastic pion scattering. It therefore appears that the theoretically predicted spin-flip E1 and M2 transitions are located in the vicinity of the giant dipole resonance.

5.2 PION SCATTERING AND CHARGE EXCHANGE ON ^{40}Ca

The nucleus ^{40}Ca is another nucleus which has long been a subject of investigation with various probes. The giant dipole

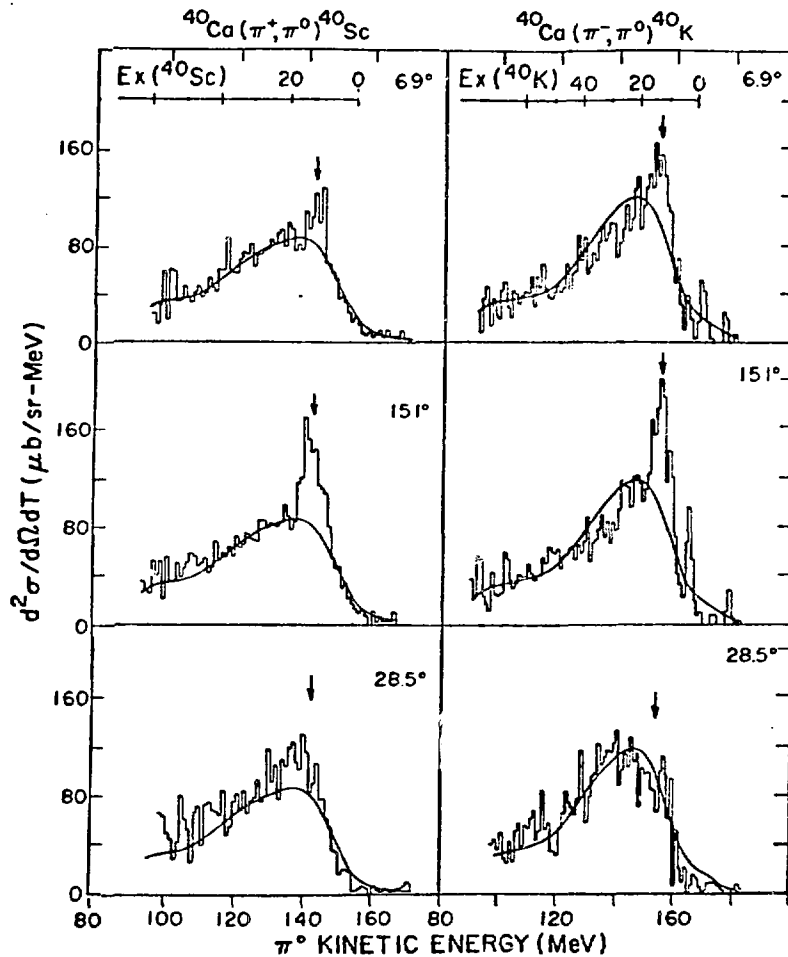


Fig. 14. π^0 spectra from $^{40}\text{Ca}(\pi, \pi^0)$ reactions studied at $T_\pi = 164$ MeV. The arrows mark the position of the analog of the GDR in ^{40}Ca . The solid line is a smoothed 4.5° spectrum drawn to facilitate observation of the GDR peak.

COMMENT
OF TEXT

resonance and isoscalar giant quadrupole resonance have both been observed at excitation energies of approximately 20 MeV in ^{40}Ca . In charge exchange reactions, the analogs of the isovector GDR are excited strongly and isoscalar transitions, of course, are forbidden, so that the GDR is not obscured. Moreover, in (p,n) reactions at 0° spin-flip transitions dominate non-spin-flip transitions, but the pion-nucleon interaction strongly favors $\Delta S = 0$ transitions at forward angles.

Spectra from $^{40}\text{Ca}(\pi^+\pi^0)$ reactions²⁶⁾ obtained with the π^0 -Spectrometer at LAMPF are shown in Fig. 14. The E1 transitions are clearly seen above the background continuum. The shift in outgoing π^0 energy between π^+ and π^- reactions results from the Coulomb displacement energy. The angular distributions for the peaks are well fitted by DWIA calculations for $1(10)$, i.e., E1, $\Delta S = 0$, transitions. A variety of forms were used for the transition density in order to estimate the collectivity of the transition. A value of approximately 2 "single particle units" was obtained. A secondary feature observable in Fig. 14 is possible broadening of the peak at 28.5° . This is interpreted as tentative evidence for the presence of spin-flip transitions, i.e., 2^- excitations.

Inelastic pion scattering²⁵⁾ by ^{40}Ca has recently been studied at extreme forward angles. In the spectra shown in Fig. 15, the prominent peaks in the lower panels are the GDR and the GOR, both natural parity transitions. The arrow in the top section indicates a peak that appears only at forward angles at the lower energy. This behavior is suggestive of a tentative identification as 1^- , $\Delta S = 1$, i.e. the $1(1,1)$ transition previously discussed for ^{12}C . Since a spin-flip is involved, the cross section would be larger at the lower energy. If the background is due to excitation of natural parity, $\Delta S = 0$ states whose cross section increase rapidly with energy, a 1^- spin-flip excitation may be easily obscured at the higher energy.

These results for pion induced reactions illustrate the versatility of pion scattering and charge exchange reactions in the investigation of even such well studied nuclei as ^{12}C and ^{40}Ca . The underlying features of the pion-nucleon interaction provides selectivity for the identification of E1, spin-flip E1, and M2 resonances even for cases where discrete states are not observed.

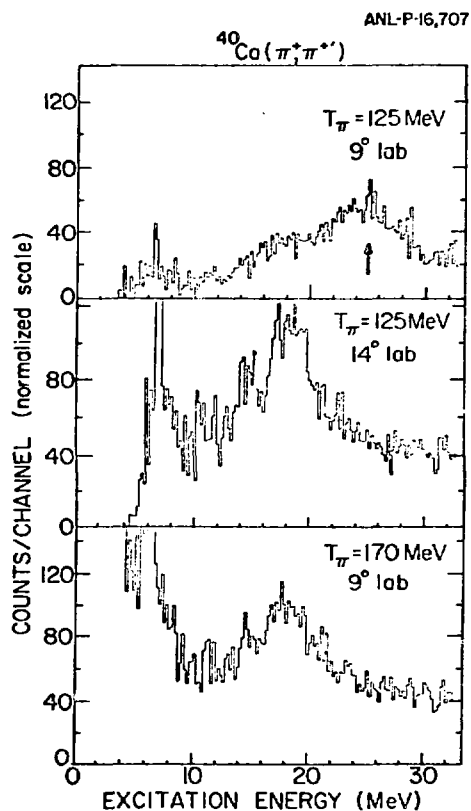


Fig. 15. Spectra from inelastic pion scattering on ^{40}Ca . The arrow indicates a peak discussed in the text.

COMMENCEMENT
OF TEXT

5.3 RECENT RESULTS OF SPECIAL INTEREST
THE FRONT PROVIDED

It would be impossible to summarize all of the recent results in pion scattering and charge exchange. In this section several particularly interesting results are presented with a minimum of discussion.

In the scattering of 125-MeV π^+ by ^{89}Y a peak is observed²⁵⁾ at forward angles at an excitation energy of approximately 8 MeV. From the angular dependence and theoretical predictions, the peak is tentatively identified as being an M1, 1(0,1), transition corresponding to the $(g_{7/2}, g_{9/2}^-)$ particle-hole configuration. Since such an excitation involves primarily neutrons, further study with π^- is planned.

The π^0 -spectrometer²⁷⁾ at LAMPF has recently become a prolific source of data. Since the spectrometer can study (π, π^0) reactions at 0° , it is uniquely capable of investigating isovector monopole transitions. Indeed, isovector monopole transitions²³⁾ have been observed in (π^-, π^0) reactions on targets of ^{90}Zr and ^{120}Sn and in the $^{120}\text{Sn}(\pi^+, \pi^0)$ reaction. Angular distributions have been measured and are found to be consistent with predicted shapes and magnitudes. In addition, these investigations have observed the giant dipole transitions. At extreme forward angles, the isobaric analog state (IAS) is prominent in the $^{120}\text{Sn}(\pi^-, \pi^0)$ spectrum.

These data are combined to produce the level diagram shown in Fig. 16. Since charge exchange may be studied with both π^+ and π^- , the isospin splitting of giant resonance structure can be inferred for excitations two units of isospin above the ground state.

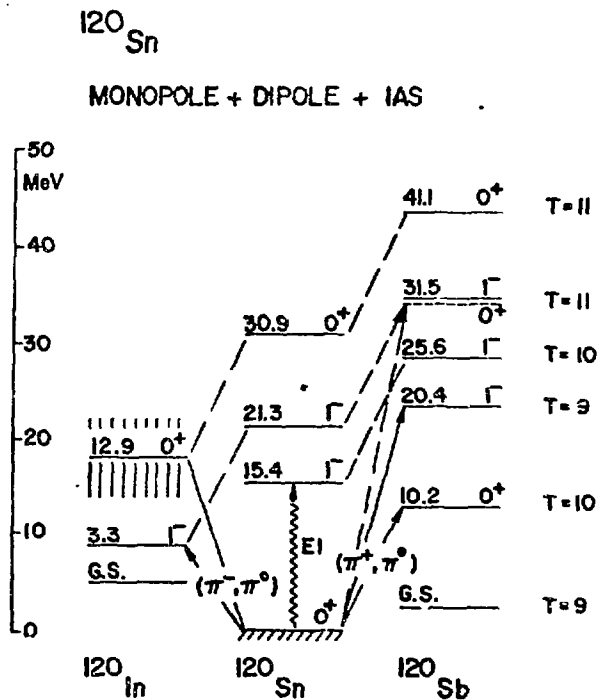


Fig. 16. Level diagram showing the measured isovector resonance built on the ^{120}Sn ground state. The energies of the $T=11$ monopole and dipole states measured for ^{120}In are projected to ^{120}Sn and ^{120}Sb using Coulomb displacement energies.

From the examples presented here, it is clear that pion scattering and charge exchange are powerful tools for investigations of nuclear structure. The properties of the π -nucleon interaction transformed into the π -nuclear system allow selective enhancement of particular aspects of nuclear structure. In the resonance region, the strong absorption simplifies the treatment of reaction mechanisms so that nuclear structure information may be emphasized. It is also clear, however, that pion induced reactions are not, in themselves, able to provide all of the nuclear structure information that is required. Data obtained in other ways or with other probes provides both complementary information and the redundant information necessary to establish the validity of results.

The approach adopted in this paper has been to utilize basic features of the π -nucleon interaction to deduce nuclear structure information. It is important to remember, however, that the approximations used are not valid at other energies or, in some cases, even on resonance. The π -nucleon interaction in nuclear matter may not be the same as on free nucleons. In other words, features of the reaction mechanism that have been neglected, may be important under some conditions. It is precisely this richness in the interaction that may in time lead to significant new discoveries concerning the structure of nuclei.

7. Acknowledgements

It is impossible to acknowledge all of the many people who have contributed data and assistance in the preparation of this paper. We particularly wish to thank L. C. Bland and H. W. Baer, for allowing us to present preliminary results and unpublished data, and D. Kurath and R. D. Lawson, for numerous discussions and calculations. We are grateful to our collaborators, too numerous to mention, and the many authors listed as "et al" in the references to unpublished material. Work supported by the U. S. Department of Energy under contract W-31-109-ENG-38.

References

- 1) D. Dehnhard, Nucl. Phys. A374 (1982) 377c; C. H. O. Ingram, Nucl. Phys. A374 (1982) 319c.
- 2) E. R. Siciliano and G. E. Walker, Phys. Rev. C 23, (1981) 2661.
- 3) T.-S. H. Lee and D. Kurath, Phys. Rev. C 21 (1980) 293; T.-S. H. Lee and D. Kurath, Phys. Rev. C 22 (1980) 1670.
- 4) A. Gal, Phys. Rev. C 25 (1982) 2680.
- 5) S. J. Seestrom-Morris, private communication.
- 6) F. Petrovich and W. G. Love, Nucl. Phys. A354 (1981) 499.
- 7) S. J. Seestrom-Morris, Los Alamos National Laboratory report LA-8916-T (1981).
- 8) LAMPF Exp. 389, B. Zeidman and G. C. Morrison, Spokesmen.
- 9) R. A. Eisenstein and F. Tabakin, Comput. Phys. Commun. 12 (1976) 237.
- 10) S. Cohen and D. Kurath, Nucl. Phys. 73 (1965) 1.
- 11) D. J. Millener and D. Kurath, Nucl. Phys. A255 (1975) 315.
- 12) I. Ragnarsson, S. Rberg, H. B. Håkansson and R. K. Sheline, Nucl. Phys. A361 (1981) 1.

COMMENCEMENT
OF TEXT

- 13) W. Knüpfner, M. Dillig and A. Richter, Phys. Lett. 93B (1980) 349.
- 14) C. Goodman, Nucl. Phys. A374 (1982) 241c.
- 15) M. Weise, Nucl. Phys. A374 (1982) 505c.
- 16) R. A. Lindgren, W. J. Gerace, A. D. Bacher, W. G. Love, and F. Petrovich, Phys. Rev. Lett. 42 (1979) 1524.
- 17) G. S. Adams et al., Phys. Rev. Lett. 38 (1977) 1387.
- 18) C. Olmer et al., Phys. Rev. Lett. 43 (1979) 612.
- 19) LAMPF Exp. 565, B. Zeidman and D. F. Geesaman, Spokesmen.
- 20) R. A. Lindgren et al., Phys. Rev. Lett. 46 (1981) 706.
- 21) R. D. Lawson, private communication.
- 22) F. Lenz, M. Thies, and Y. Horikawa, to be published.
- 23) H. W. Baer, contributed paper, this conference.
- 24) C. F. Moore, C. J. Harvey, C. L. Morris, S. J. Greene, D. Holtkamp, and H. T. Fortune, Phys. Rev., to be published.
- 25) LAMPF Exp. 659, L. C. Bland, Spokesman.
- 26) H. W. Baer et al., to be published.
- 27) H. W. Baer et al., Nucl. Instrum. Meth. 180 (1981) 445.

DISCLAIMER

This report was prepared as an account of work sponsored by an agency of the United States Government. Neither the United States Government nor any agency thereof, nor any of their employees, makes any warranty, express or implied, or assumes any legal liability or responsibility for the accuracy, completeness, or usefulness of any information, apparatus, product, or process disclosed, or represents that its use would not infringe privately owned rights. Reference herein to any specific commercial product, process, or service by trade name, trademark, manufacturer, or otherwise does not necessarily constitute or imply its endorsement, recommendation, or favoring by the United States Government or any agency thereof. The views and opinions of authors expressed herein do not necessarily state or reflect those of the United States Government or any agency thereof.